

## Flexible Eightfold Interpenetrating Diamondoid Network Generating 1D Channels: Selective Binding with Organic Guests

Hyunji Kim and Myunghyun Paik Suh\*

School of Chemistry, Seoul National University, Seoul 151-747, Republic of Korea

Received August 17, 2004

An 8-fold interpenetrating diamondoid network,  $[\text{Ni}(\text{cyclam})]_2[\text{TCM}] \cdot 2\text{DMF} \cdot 10\text{H}_2\text{O}$ , has been prepared by the self-assembly of a Ni(II)cyclam macrocyclic complex and sodium tetrakis[4-(carboxyphenyl)oxamethyl]methane in DMF/water. The network shows an unusual [4 + 4] mode of interpenetration, generating 1D channels of effective window size  $6.7 \text{ \AA} \times 4.7 \text{ \AA}$ . The network shows flexible behavior: it becomes nonporous on removal of the guest molecules occupying the channels, but the open structure is restored when the desolvated solid is immersed in the mixture of  $\text{H}_2\text{O}/\text{DMF}$  (1:1, v/v) for 5 min. The desolvated host has different binding capacities for *n*-butanol, pyridine, and ethanol.

Assembly of metal–organic open frameworks (MOFs) has attracted great attention, and MOFs with various network topologies have been prepared from the metal and organic building blocks.<sup>1–5</sup> They have the potential for being applied to selective molecular recognition and separation,<sup>2</sup> gas storage,<sup>3</sup> ion-exchange,<sup>4</sup> and heterogeneous catalysis.<sup>5</sup> It is of interest to build diamondoid networks with big cavities because they have the perspective to be used as porous materials or for a catalytic purpose. Interpenetrating diamondoid networks with open structures including counterions and guest molecules have been demonstrated.<sup>6–8</sup>

Our design strategy was to build a neutral diamondoid network by interconnecting a big pseudotetrahedral anionic ligand and a metal ion having two coordination sites at the trans position (Scheme 1). We chose tetrakis[4-(carboxyphenyl)oxamethyl]methane (TCM) ligand<sup>9</sup> as the tetradentate organic building block and Ni(II)cyclam<sup>10</sup> macrocyclic complex as the metal building block. Macrocyclic complexes have been rarely employed as metal building blocks in the assembly of metal–organic frameworks,<sup>2,11–13</sup> mainly because of the difficulty of synthesis and weak ligand binding affinity at the axial sites. However, they have advantages over the free metal ions. Macrocyclic complexes in square planar coordination geometry can act as the linear linkers for the ligand, and thus make the design and prediction of the networks possible. In addition, bulkiness of the macrocycle often prevents interpenetration of the network. Interpenetration is a major impediment in the achievement of channels or cavities in MOFs even though it occasionally provides open structures.<sup>13–15</sup>

Self-assembly of  $[\text{Ni}(\text{cyclam})](\text{ClO}_4)_2$  and  $\text{Na}_4\text{TCM}$  in DMF/water (1:1, v/v) resulted in  $[\text{Ni}(\text{cyclam})]_2[\text{TCM}] \cdot 2\text{DMF} \cdot 10\text{H}_2\text{O}$  (**1**).<sup>16</sup> Compound **1** is insoluble in water and common organic solvents. The crystal retains transparency even after exposure to air.

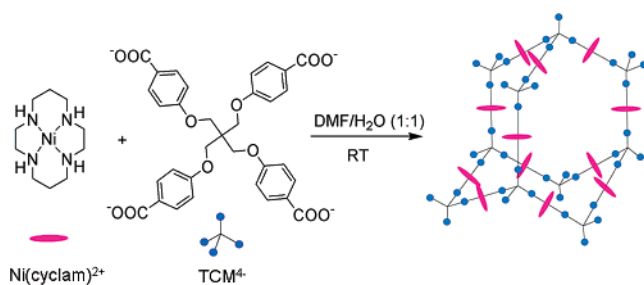
In the X-ray crystal structure of **1**,<sup>17</sup> each Ni(II) ion is coordinated with two different TCM ligands at the axial sites to display distorted octahedral coordination geometry, and each TCM ligand binds four Ni(II)cyclam complexes in a tetrahedral fashion, which gives rise to a diamondoid network

\* To whom correspondence should be addressed. E-mail: mpsuh@snu.ac.kr.

- (1) (a) Kitagawa, S.; Kitaura, R.; Noro, S. *Angew. Chem., Int. Ed.* **2004**, *43*, 2334–2375. (b) Eddaoudi, M.; Moler, D. B.; Li, H.; Chen, B.; Reineke, T. M.; O’Keeffe, M.; Yaghi, O. M. *Acc. Chem. Res.* **2001**, *34*, 319–330.
- (2) (a) Choi, H. J.; Suh, M. P. *J. Am. Chem. Soc.* **2004**, *126*, 15844–15851. (b) Lee, E. Y.; Suh, M. P. *Angew. Chem., Int. Ed.* **2004**, *43*, 2798–2801. (c) Ko, J. W.; Min, K. S.; Suh, M. P. *Inorg. Chem.* **2002**, *41*, 2151–2157. (d) Min, K. S.; Suh, M. P. *Chem. Eur. J.* **2001**, *7*, 303–313. (e) Choi, H. J.; Lee, T. S.; Suh, M. P. *Angew. Chem., Int. Ed.* **1999**, *38*, 1405–1408.
- (3) (a) Eddaoudi, M.; Kim, J.; Rosi, N.; Vodak, D.; Wachter, J.; O’Keeffe, M.; Yaghi, O. M. *Science* **2002**, *295*, 469–472. (b) Rosi, N. L.; Eckert, J.; Eddaoudi, M.; Vodak, D. T.; Kim, J.; O’Keeffe, M.; Yaghi, O. M. *Science* **2003**, *300*, 1127–1129.
- (4) Min, K. S.; Suh, M. P. *J. Am. Chem. Soc.* **2000**, *122*, 6834–6840.
- (5) Seo, J. S.; Whang, D.; Lee, H.; Jun, S. I.; Oh, J.; Jeon, Y. J.; Kim, K. *Nature* **2000**, *404*, 982–986.
- (6) Carlucci, L.; Ciani, G.; Proserpio, D. M.; Rizzato, S. *Chem. Eur. J.* **2002**, *8*, 1519–1526.
- (7) (a) Klein, C.; Graf, E.; Hosseini, M. W.; Cian, A. D. *New J. Chem.* **2001**, *25*, 207–209.

- (8) (a) Liu, Y.; Wu, H.; Lin, H.; Hou, W.; Lu, K. *Chem. Commun.* **2003**, 60–61. (b) Blatov, V. A.; Carlucci, L.; Ciani, G.; Proserpio, D. M. *CrystEngComm* **2004**, *6*, 377–395. (c) Batten, S. R.; Robson, R. *Angew. Chem., Int. Ed.* **1998**, *37*, 1460–1495.
- (9) Oike, H.; Imamura, H.; Imaizumi, H.; Tezuka, Y. *Macromolecules* **1999**, *32*, 4819–4825.
- (10) Barefield, E. K.; Wagner, F.; Herlinger, A. W.; Dahl, A. R. *Inorg. Synth.* **1976**, *220*.
- (11) Choi, H. J.; Suh, M. P. *J. Am. Chem. Soc.* **1998**, *120*, 10622–10628.
- (12) Suh, M. P.; Ko, J. W.; Choi, H. J. *J. Am. Chem. Soc.* **2002**, *124*, 10976–10977.
- (13) Suh, M. P.; Choi, H. J.; So, S. M.; Kim, B. M. *Inorg. Chem.* **2003**, *42*, 676–678.
- (14) Chen, B.; Eddaoudi, M.; Hyde, S. T.; O’Keeffe, M.; Yaghi, O. M. *Science* **2001**, *291*, 1021–1023.
- (15) Reineke, T. M.; Eddaoudi, M.; Moler, D.; O’Keeffe, M.; Yaghi, O. M. *J. Am. Chem. Soc.* **2000**, *122*, 4843–4844.

Scheme 1



formed of large adamantanoid cages. The adamantanoid cage exhibits maximum dimensions (the longest intracage distances) of  $49.2 \times 50.8 \times 44.3 \text{ \AA}^3$  (C···C edges;  $20.9 \text{ \AA}$ ) (Figure 1). Such a large cavity causes the unusual 8-fold interpenetration of the networks, which can be best described as two sets of a normal 4-fold net. The two sets are related to a noncrystallographic 2-fold rotation, whose axis lies in the middle of two sets and on the *ac* plane. The interpenetration vector in each set is along the *a* + *c*. Therefore, this interpenetration is rototranslational equivalent, and compound **1** is regarded as a [4 + 4] interpenetrating diamondoid system.<sup>6</sup>

Despite the 8-fold interpenetration, the structure generates 1D channels of effective window size  $6.7 \text{ \AA} \times 4.7 \text{ \AA}$ . The channels are filled with guest molecules, 2 DMF and 10 water molecules per unit formula of the host, as evidenced by the elemental analysis and TGA/DSC data. In the X-ray structure refinement, however, guest molecules could not be located because of their high thermal disorder, and the final structural model was refined without the solvent molecules by using a SQUEEZE routine of PLATON.<sup>18</sup> The voids volume estimated by PLATON is 30.1%. TGA data obtained for the freshly prepared sample indicate that all guest molecules can be removed at 30–105 °C, and the guest-free framework is stable up to 320 °C.

The X-ray powder diffraction (XRPD) pattern of desolvated solid **2** shows sharp peaks, but it is different from that of original solid **1** (Figure 2). This indicates that the crystal structure was changed by the guest removal. The N<sub>2</sub> gas

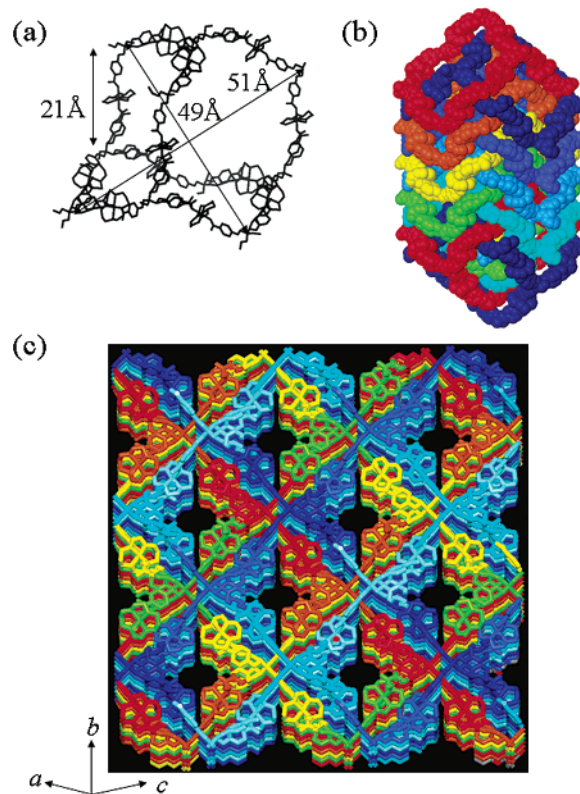


**Figure 1.** X-ray structure of **1**. (a) An adamantanoid cage. (b) The [4 + 4] interpenetrating mode of diamondoid networks. (c) View on the (101) plane, showing that the interpenetrating networks generate 1D channels (effective window size,  $6.7 \text{ \AA} \times 4.7 \text{ \AA}$ ). One set of the [4 + 4] interpenetrating networks is indicated in red, brick, yellow, and green, the other set is in indigo, blue, sky blue, and light blue.

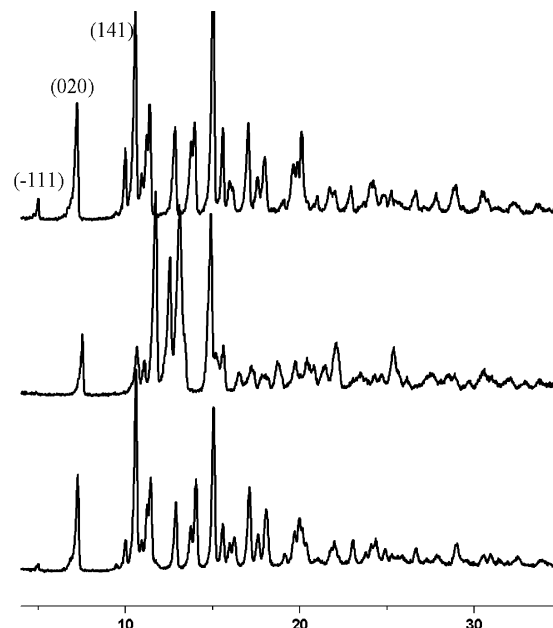


**Figure 2.** XRPD patterns for original solid **1** (top), desolvated solid **2** prepared at 120 °C and  $10^{-5}$  Torr for 20 h (middle), and resolvated solid by immersion of **2** in H<sub>2</sub>O/DMF (1/1, v/v) for 5 min (bottom).

sorption study indicates that the desolvated solid became nonporous. However, when the desolvated solid was immersed in the mixture of H<sub>2</sub>O/DMF (1:1, v/v) for 5 min, the same pattern as that of the original crystal was obtained, indicating that the original structure was restored upon

(16) Synthesis of **1**: The nickel(II) cyclam complex (60 mg,  $1.30 \times 10^{-4}$  mol) was dissolved in *N,N*-dimethylformamide (5 mL). The solution was allowed to diffuse into the mixture of *N,N*-dimethylformamide and water (3:7 v/v, 10 mL) containing sodium tetrakis[4-(carboxyphenyl)oxamethyl]methane (50 mg,  $6.50 \times 10^{-5}$  mol). The solution was allowed to stand at room temperature for several days until pale violet crystals formed, which were filtered off, washed with water, and dried in air. Yield: 0.082 g, 87%. UV/vis (diffuse reflectance spectrum,  $\lambda_{\text{max}}$ ): 513, 717, and 796 nm. Anal. Calcd for Ni<sub>2</sub>C<sub>59</sub>H<sub>106</sub>N<sub>10</sub>O<sub>24</sub>: C, 48.64; H, 7.33; N, 9.61. Found: C, 48.99; H, 7.23; N, 9.67.

(17) Crystal data for **1**: Ni<sub>2</sub>C<sub>59</sub>H<sub>106</sub>N<sub>10</sub>O<sub>24</sub>,  $M_w = 1456.95$ , monoclinic, space group *P2<sub>1</sub>/c* (No. 14),  $a = 33.593(2) \text{ \AA}$ ,  $b = 24.577(1) \text{ \AA}$ ,  $c = 33.657(2) \text{ \AA}$ ,  $\beta = 97.711(1)^\circ$ ,  $V = 27537(2) \text{ \AA}^3$ ,  $Z = 4$ ,  $T = 258 \text{ K}$ ,  $\mu(\text{Mo K}\alpha) = 0.641 \text{ mm}^{-1}$ , 28988 reflections measured, final  $R_1$  and  $wR_2$  values 0.0925 and 0.2251 for 9769 independent reflections [ $I > 2\sigma(I)$ ]. A pale violet needle crystal of **1** was sealed in a glass capillary with mother liquor and mounted on an Enraf Nonius Kappa CCD diffractometer equipped with a normal focus Mo-target X-ray tube ( $\lambda = 0.71073 \text{ \AA}$ ), within the limits  $1.03^\circ < \theta < 20.92^\circ$ . The structure was solved by direct methods and the subsequent difference Fourier syntheses, and refined with the *SHELXTL* (version 6.10) software package.

(18) Spek, A. L. *PLATON, A Multipurpose Crystallographic Tool*; Utrecht University: Utrecht, The Netherlands, 2003.

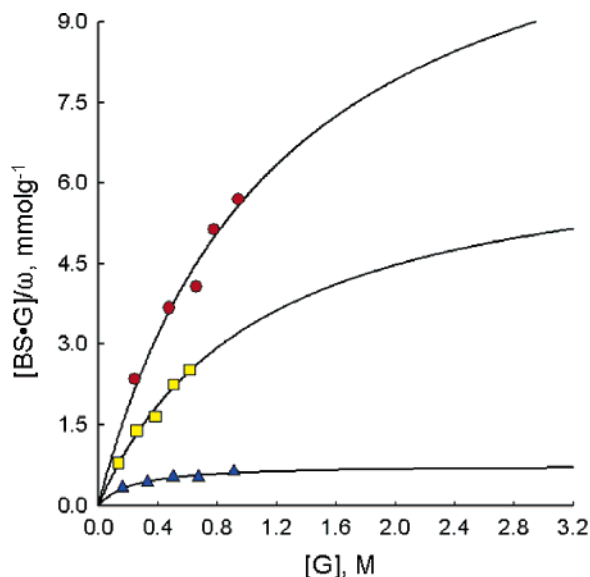


**Figure 3.** Binding of desolvated solid **2** (in the powder form) with various guest molecules in the isoctane medium, ethanol (●), pyridine (■), and *n*-butanol (▲).

resolution. However, when the desolvated solid was exposed for 7 days to the vapor of DMF and H<sub>2</sub>O (10:1.8, v/v) mixture, whose partial vapor pressure ratio is DMF/H<sub>2</sub>O = 1:5 at 38 °C, the XRPD pattern of the desolvated solid was not changed. This implies that the desolvated structure cannot adsorb the vapor, which is in accordance with the N<sub>2</sub> gas sorption results. These types of flexible and dynamic networks responding to guest molecules have been reported,<sup>12,19,20</sup> and they might find applications in molecular separation or sensors. In particular, our result that nonporous solid **2** readily adsorbs guest solvents with structural change is similar to Atwood's report that the nonporous calixarene solid transports solvent molecules rapidly with significant positional and orientational rearrangement of the host molecules.<sup>20</sup>

Desolvated host solid **2** is able to differentiate various organic guests in the isoctane medium. It binds ethanol, pyridine, and *n*-butanol, exhibiting Langmuir isotherm curves (Figure 3), while it does not bind toluene and *tert*-butanol. The amount of organic guest molecules bound to the solid was measured by GC at various guest concentrations, and the host–guest complex formation constant ( $K_f$ ) and the

**Table 1.** Guest Binding Data for Desolvated Host **2**<sup>a,b</sup>

	$K_f$ , M <sup>-1</sup>	[BS] <sub>0</sub> /ω, mmol g <sup>-1</sup>	guest inclusion capacity, <sup>c</sup> mol
ethanol	0.84 ± 0.36	12.7 ± 3.4	14.4
pyridine	0.93 ± 0.36	6.87 ± 1.84	7.81
<i>n</i> -butanol	4.36 ± 1.22	0.75 ± 0.07	0.85

<sup>a</sup> Measurements were performed according to the method in ref 2. <sup>b</sup>  $K_f$  and [BS]<sub>0</sub>/ω indicate the binding constant and the binding capacity of host solid with guest molecules, respectively. <sup>c</sup> Per formula unit of desolvated host **2** (fw = 1136).

number of binding sites (moles) per gram of the host ([BS]<sub>0</sub>/ω) for guest molecules were estimated (Table 1). The  $K_f$  values indicate that the host binds guests in the order *n*-butanol > pyridine > ethanol. This indicates that the guest should interact with the host via hydrogen bonding interactions with the carbonyl group of TCM or with secondary amine of the macrocycle. In addition, hydrophobic interactions between the host and guest are also very important because macrocycles are exposed to the channels (Figure 1), as indicated by the largest  $K_f$  value for *n*-butanol. As anticipated, the maximum amount of guest molecules that can be bound to the host depends on the size of the guest.

In conclusion, the uncommon 8-fold [4 + 4] interpenetrating diamondoid network has been assembled from a Ni(II)-cyclam complex and tetra-carboxylate ligand. Despite of the highfold interpenetration, the network generates a 1D channel. The network exhibits dynamic behavior: it becomes nonporous on removal of guest molecules, but the original open structure is restored upon immersion in the guest solvent system for 5 min. The desolvated host solid has different binding capacities for *n*-butanol, pyridine, and ethanol. A variety of aza-macrocyclic complexes can be prepared by attaching various functional groups to the macrocycles.<sup>21</sup> By employing them as the metal building blocks, we are now preparing different types of networks, which might show high specificity for particular guests.

**Acknowledgment.** This work was supported by the Korea Institute of Science & Technology Evaluation and Planning (Project M1-0213-03-0001). We thank Prof. Proserpio for helpful discussion.

**Supporting Information Available:** ORTEP drawing, TGA/DSC plot, tables of crystallographic data, and an X-ray crystallographic file in CIF format for **1**. This material is available free of charge via the Internet at <http://pubs.acs.org>.

IC048869W

(19) Kitaura, R.; Seki, K.; Akiyama, G.; Kitagawa, S. *Angew. Chem., Int. Ed.* **2003**, *42*, 428–431.

(20) Atwood, J. L.; Barbour, L. J.; Jerga, A.; Schottel, B. L. *Science* **2002**, *298*, 1000–1002.

(21) Suh, M. P. *Adv. Inorg. Chem.* **1997**, *44*, 93–146.